PHYSICAL REVIEW A VOLUME 52, NUMBER 5 NOVEMBER 1995

Comparison of eikonal and multiple-scattering representations of internuclear scattering in charge transfer at forward angles

Steven Alston*

Physics Department, Pennsylvania State University, Wilkes-Barre Campus, Lehman, Pennsylvania 18627
and Theoretical Physics, University of Tennessee, Knoxville, Tennessee 37996

(Received 21 December 1994)

In near-symmetric charge transfer at high-impact velocities and forward-scattering angles, the internuclear-scattering component of the second-order Faddeev representation of the generalized Thomas mechanisms, which, though generally associated with large-angle scattering, is valid at forward angles also, has been shown previously to agree with both the eikonal treatment in a continuum distorted-wave theory and the experimental data. A comparison of the multiple-scattering and eikonal methods using the same electronic amplitude is made in this paper. Significant differences are found between the results of the two methods, especially in the region where there is substantial cancellation among the partial amplitudes. At high velocities the Faddeev amplitude is a factor of 2 larger than the eikonal amplitude, a result attributable to the inclusion of *two* generalized Thomas channels in the former. The leading asymptotic form of the amplitude is also given.

PACS number(s): 34.70.+e

I. INTRODUCTION

At projectile energies of a few MeV, a second-order Faddeev treatment of charge transfer [1] has been shown to agree well with the experimental differential cross section in proton-helium and proton-hydrogen collisions [2]. For these energies, multiple-scattering contributions play a significant role due to the importance of the Thomas double-scattering mechanism [3]. The Faddeev scattering formalism [4,5] involves a theoretical decomposition of the entire collision process into two-body collisions treated using the corresponding two-body transition operators. The Faddeev treatment maintains the simple description of the Thomas mechanisms in the second-order Born treatment while providing quantitative agreement with the experimental data, which the latter does not give. At projectile scattering angles beyond the Thomas peak (at 0.47 mrad) where nuclear scattering is the main effect, the agreement with experiment is maintained because the internuclear interaction is included in the Faddeev treatment.

In the present paper, to study the Faddeev internuclear contribution in more detail, a comparison with the eikonal treatment is made for proton-hydrogen and proton-helium collisions at two sets of incident energies, corresponding to velocities of five and ten times the characteristic target orbital velocities. A simple method for inclusion of the contribution of the internuclear potential is the eikonal transform [6]. A general application, for projectile and target nuclear charges Z_P and Z_T and velocity v, proceeds by transforming the electronic amplitude in the wave picture over to impact parameter space b, multiplying the transformed amplitude by the eikonal phase factor $b^{2iZ_PZ_T/v}$, which derives from the transverse components of the internuclear motion, and then transforming this amplitude back to the wave picture.

An exact numerical evaluation of the Faddeev amplitude is not critical to the comparison presented here and is not attempted. Rather, an approximate treatment is used which relies on the smallness of the binding energy of the electron relative its final kinetic energy. Near-the-energy-shell representations of the two-body transition matrices are employed and, further, factors which introduce errors of the order of the electron mass to the heavy-particle masses are neglected [1].

The plan of the paper is as follows. The second-order Faddeev amplitude is specified in Sec. II, including both the electronic and internuclear parts. In Sec. III A, the partial amplitudes are either evaluated to a closed form or reduced to a numerically tractable form; in Sec. III B, the eikonally transformed amplitude is defined; and in Sec. III C, the high-velocity limit of the internuclear part of the Faddeev amplitude is derived. Section IV presents a comparison of calculated results along with a comparative analysis. Atomic units are used. The normalization used is such that a plane-wave state of momentum $\mathbf{k}$ in coordinate space $\mathbf{r}$ is $\phi_{\mathbf{k}}(\mathbf{r})=e^{i\mathbf{k}\cdot\mathbf{r}}$.

II. SECOND-ORDER FADDEEV AMPLITUDE

Consider a three-body collision in a one-electron model in which a projectile ion P is incident on a target consisting of an electron e and a target ion T. The target or projectile may contain nonactive electrons. Accordingly, the two-body interactions between pairs of particles assume general modified Coulomb forms. A detailed account of the application of the Faddeev formalism to the charge transfer problem is given elsewhere [1]; only a few parts relevant to the present treatment are reiterated. Working to divide the full collision into two-body components, Faddeev obtained a set of coupled equations for channel operators based on the two-body interactions [4]. A second-order approximate solution of the equations is employed here. After introducing Fourier analyses of the initial and final bound-state wave functions and integrating the heavy-particle motion, an amplitude containing two-body transition matrices T is obtained. These transition matrices are subsequently approximated by near-the-energy-shell forms.

*On sabbatical from The Pennsylvania State University, Wilkes-Barre Campus, Lehman, PA 18627.

The second-order Faddeev amplitude A_{F2} consists of an *electronic* part A_e independent of the internuclear interaction and an inter*nuclear* part A_n dependent on it:

$$A_{F2} \equiv A_e + A_n \, . \tag{1}$$

In the electronic part, the double-scattering term is separated giving

$$A_e = A_{B1} + A_e^{(2)} , \tag{2}$$

where A_{B1} is the first Born amplitude. For the partial amplitude A_n, the first-order part is split off as well,

$$A_n = A_n^{(1)} + A_n^{(2a)} + A_n^{(2b)} , \tag{3}$$

with the superscript number in this and the previous equations denoting the number of separate interactions.

The first Born amplitude has the form

$$A_{B1} = (2\pi)^{3/2} \int d\mathbf{k}_f d\mathbf{k}_i [\tilde{\phi}_f(\mathbf{k}_f)]^* \tilde{\phi}_i(\mathbf{k}_i) \times \tilde{V}_{Pe}(\mathbf{k}_f - \mathbf{K}) \, \delta(\mathbf{k}_i + \mathbf{J}) , \tag{4}$$

where $\delta(\mathbf{k}_i + \mathbf{J})$ is the three-dimensional Dirac delta function. The second-order partial amplitude in Eq. (2) has the form

$$\begin{aligned} A_e^{(2)} = (2\pi)^{-3} \int & d\mathbf{k}_f d\mathbf{k}_i [\tilde{\phi}_f(\mathbf{k}_f)]^* \tilde{\phi}_i(\mathbf{k}_i) \\ & \times T_{Te}(\mathbf{k}_f + \mathbf{v}, \mathbf{k}_i + \mathbf{k}_f - \mathbf{K}; E_f) \tilde{G}_0^+(E_i) \\ & \times T_{Pe}(\mathbf{k}_f + \mathbf{k}_i + \mathbf{J}, \mathbf{k}_i - \mathbf{v}; E_i) . \end{aligned} \tag{5}$$

The two-body transition matrix is defined as

$$T(\mathbf{k}', \mathbf{k}; \varepsilon) \equiv \left\langle \mathbf{k}' \middle| V \left[1 + \left\{ \varepsilon + \frac{1}{2\mu} \nabla_{\mathbf{r}}^2 - V + i\eta \right\}^{-1} V \right] \middle| \mathbf{k} \right\rangle \tag{6}$$

for a potential V. The transition matrices T_{Pe} and T_{Te} in Eq. (5) derive, respectively, from the potentials V_{Pe} and V_{Te}; they are completely off the energy shell: $k^2 \neq 2\mu\varepsilon$ and $k'^2 \neq 2\mu\varepsilon$ with μ denoting μ_i for T_{Te} or μ_f for T_{Pe}. The free Green function can assume either of two equivalent forms:

$$\begin{aligned} \tilde{G}_0^+(E_i) &= [E_i - \tfrac{1}{2}(\mathbf{k}_i + \mathbf{k}_f + \mathbf{J})^2 + i\eta]^{-1} \\ &= [E_f - \tfrac{1}{2}(\mathbf{k}_i + \mathbf{k}_f - \mathbf{K})^2 + i\eta]^{-1} , \end{aligned} \tag{7}$$

which are useful later.

The total energy of the system is given by $E = (1/2\nu_i)K_i^2 + \varepsilon_i = (1/2\nu_f)K_f^2 + \varepsilon_f$, where ε_i and ε_f are the initial and final bound-state energies. Initial, final, and internuclear internal and relative reduced masses and associated mass ratios for the two-body combinations are defined as $\mu_i = mM_T/(m+M_T)$, $\nu_i = M_P(m+M_T)/(m+M_P+M_T)$, $\alpha = M_T/(m+M_T)$, $\mu_f = mM_P/(m+M_P)$, $\nu_f = M_T(m+M_P)/(m+M_P+M_T)$, $\beta = M_P/(m+M_P)$, $\mu_n = M_P M_T/(M_P+M_T)$, $\nu_n = m(M_T+M_P)/(m+M_P+M_T)$, and $\gamma = M_T/(M_P+M_T)$, respectively. (M_P, M_T, and m are the projectile, target-nuclear, and electronic masses.) Initial and final heavy-particle velocities are defined using the wave vectors: $\mathbf{v}_i = \mathbf{K}_i/\nu_i$ and $\mathbf{v}_f = \mathbf{K}_f/\nu_f$. To order m/M_P and m/M_T, $\alpha \approx 1$ and $\beta \approx 1$, and one can show for forward-angle capture that $v_f/v_i \approx 1$ and $\mathbf{v}_f \cdot \mathbf{v}_i \approx 1$; thus the velocity is written simply as $\mathbf{v}$. Similarly, the scattering energies in Eq. (5) are $E_i \approx \frac{1}{2}v^2 - \mathbf{v} \cdot \mathbf{k}_i + \varepsilon_i$ and $E_f \approx \frac{1}{2}v^2 + \mathbf{v} \cdot \mathbf{k}_f + \varepsilon_f$. The momenta transferred to the target ion and projectile during the collision are $\mathbf{J} = \alpha \mathbf{K}_i - \mathbf{K}_f$ and $\mathbf{K} = \beta \mathbf{K}_f - \mathbf{K}_i$. The components parallel to $\mathbf{v}$ are $K_z = -v/2 + (\varepsilon_i - \varepsilon_f)/v$ and $J_z = -v/2 + (\varepsilon_f - \varepsilon_i)/v$, and those perpendicular to it are $K_\perp$ for $\mathbf{K}$ and $-K_\perp$ for $\mathbf{J}$. Momentum conservation takes the form $\mathbf{K} + \mathbf{J} + \mathbf{v} = \mathbf{0}$.

Equation (5) represents an electronic "wave packet" of momentum distribution $\tilde{\phi}_i(\mathbf{k}_i)$ centered about $-\mathbf{v}$ scattering in the projectile frame. The energy of each component is $E_i(\mathbf{k}_i)$. In the collision with the projectile, each component of the packet suffers a momentum transfer of $\mathbf{k}_f - \mathbf{K}$, as described by the transition matrix T_{Pe}. After free propagation (represented by $\tilde{G}_0^+$), the packet, as seen now from the target frame, scatters off the target ion with each component suffering a momentum transfer of $-\mathbf{k}_i - \mathbf{J}$. The second scattering is described by the transition matrix T_{Te}. The final momentum distribution is $\tilde{\phi}_f(\mathbf{k}_f)$ about $\mathbf{v}$ with energy $E_f(\mathbf{k}_f)$ for each component.

For the internuclear part of the amplitude, the first-order term in Eq. (3) is

$$\begin{aligned} A_n^{(1)} = \int & d\mathbf{k}_f d\mathbf{k}_i [\tilde{\phi}_f(\mathbf{k}_f)]^* \tilde{\phi}_i(\mathbf{k}_i) \\ & \times T_{PT}(\mathbf{U}_i - \mathbf{k}_f + \mathbf{K}, \mathbf{U}_i; E_n) \, \delta(\mathbf{k}_f - \mathbf{k}_i + \mathbf{v}) , \end{aligned} \tag{8}$$

where $\mathbf{U}_i = (1-\gamma)\mathbf{k}_i + [1 - (1-\gamma)(1-\alpha)]\mathbf{K}_i \approx \mu_n \mathbf{v}$ and $E_n = E - [\mathbf{k}_i - (1-\alpha)\mathbf{K}_i]^2/2\nu_n$. This term represents a contribution of internuclear scattering either of momentum transfer $-\mathbf{k}_i - \mathbf{J}$ for bound-state (electronic) momenta $\mathbf{k}_i \approx \mathbf{0}$ in ϕ_i and $\mathbf{k}_i \approx \mathbf{v}$ in ϕ_f, or of momentum transfer $\mathbf{k}_i - \mathbf{K}$ for bound-state momenta $\mathbf{k}_i \approx -\mathbf{v}$ in ϕ_i and $\mathbf{k}_i \approx \mathbf{0}$ in ϕ_f. [See also after Eq. (22).]

For the first of the second-order terms in Eq. (3) one obtains the expression

$$\begin{aligned} A_n^{(2a)} = (2\pi)^{-3} \int & d\mathbf{k}_f d\mathbf{k}_i [\tilde{\phi}_f(\mathbf{k}_f)]^* \tilde{\phi}_i(\mathbf{k}_i) \\ & \times T_{Te}(\mathbf{k}_f + \mathbf{v}, \mathbf{k}_i - (1-\alpha)(\mathbf{k}_f - \mathbf{K}); E_f) \, \tilde{G}_0^+(E_f) \\ & \times T_{PT}(\mathbf{U}_i - \mathbf{k}_f + \mathbf{K}, \mathbf{U}_i; E_n) . \end{aligned} \tag{9}$$

The momentum-space Green function in Eq. (9) is given by

$$\tilde{G}_0^+(E_f) = \left(E_f - \frac{1}{2\mu_i} [\mathbf{k}_i + (1-\alpha)(\mathbf{K} - \mathbf{k}_f)]^2 + i\eta \right)^{-1} . \tag{10}$$

The picture represented by Eq. (9) is that of scattering via a so-called generalized Thomas double-scattering mechanism [3]: the projectile and target nucleus scatter (T_{PT}) and then the electron and target nucleus scatter (T_{Te}). The projectile of momentum $\mathbf{U}_f \approx \mu_n \mathbf{v}$ suffers the small momentum transfer of $\mathbf{k}_f - \mathbf{K}$ while the electron, initially of momentum $\mathbf{k}_i$, ends up with momentum $\mathbf{k}_f+\mathbf{v}$. Thus, the electron and projectile travel in the end with nearly the same velocity, allowing capture to occur. Originally, this mechanism was used to argue for the possibility of an enhanced cross section at projectile scattering angle of about 60°; however, because of the momentum spread in the bound-state wave functions, the mechanisms can work at any angle, in particular, at forward angles.

Similarly, for the second of the second-order terms in Eq. (3), one finds

$$A_n^{(2b)}=(2\pi)^{-3}\int d\mathbf{k}_f d\mathbf{k}_i[\tilde{\phi}_f(\mathbf{k}_f)]^*\tilde{\phi}_i(\mathbf{k}_i) \times T_{PT}(\mathbf{U}_f,\mathbf{U}_f+\mathbf{k}_i+\mathbf{J};E_n)\ \tilde{G}_0^+(E_i) \times T_{Pe}(-\mathbf{k}_f+(1-\beta)(\mathbf{k}_i+\mathbf{J}),\mathbf{k}_i-\mathbf{v};E_i). \quad (11)$$

with $\mathbf{U}_f=-\gamma\mathbf{k}_f+[1-\gamma(1-\beta)]\mathbf{K}_f$. The momentum-space Green function is given by

$$\tilde{G}_0^+(E_i)=\left(E_i-\frac{1}{2\mu_f}[-\mathbf{k}_f+(1-\beta)(\mathbf{k}_i+\mathbf{J})]^2+i\eta\right)^{-1}. \quad (12)$$

In this double-collision term, the electron and projectile scatter (T_{Pe}) and then the projectile and target nucleus scatter (T_{PT}). The electron, initially of momentum $\mathbf{k}_i-\mathbf{v}$ (in the projectile frame), ends up with momentum $\mathbf{k}_f$, and the projectile of momentum $\mathbf{U}_f\approx\mu_n\mathbf{v}$ suffers the small momentum transfer of $-\mathbf{k}_i-\mathbf{J}$. Again, both the electron and projectile end up with almost the same velocity so that capture occurs.

The interference of the two terms of Eqs. (9) and (11) together with that of Eq. (8) produces the nuclear scattering. It happens that, to good approximation, the electronic and nuclear scattering decouple as in Eq. (21) below, but it is the proper treatment of both the off-shell and Coulomb aspects of the scattering which leads to a nonzero contribution—a second Born treatment gives a vanishing contribution. The amplitude specified in Eqs. (4), (5), (8), (9), and (11) contains only errors of the order of m/M_P or m/M_T. Finally, on noting that $\tilde{G}_0^+\sim v^{-2}$, one sees that Eqs. (4) and (5) lead to a momentum dependence of $v^{-2}Q^{-4}$ whereas Eqs. (8), (9), and (11) lead to a dependence of $v^{-4}Q^{-2}$, where Q is J or K. Therefore, beyond a certain value of $K_\perp$, the internuclear terms will dominate.

III. EVALUATION OF THE AMPLITUDE

A. Near-shell approximation to the amplitude

The partial amplitude for A_{F2} given in Eq. (5) is approximated to order $(Z_P/v)^2$ and $(Z_T/v)^2$. For a modified Coulomb (MC) potential and scattering near the energy shell, the two-body transition matrix reduces to a generalized elastic scattering amplitude multiplied by a so-called off-energy-shell factor. The generalized elastic scattering amplitude is the sum of Coulomb and short-range amplitudes. Because of the presence of the bound-state wave functions, the integral in the second-order electronic term is dominated by momentum values in the regions $k_i\lesssim Z_T$ and $k_f\lesssim Z_P$. Following previous work on modified Coulomb potentials [7], and noting that the modified Coulomb potential is represented well by a scaled pure Coulomb potential of charge Z_s in the inner region, the sum of the Coulomb and short-range amplitudes is approximated by the Coulomb amplitude for the screened potential [8]. Thus, the near-the-energy-shell approximation to the two-body scattering matrix Eq. (6) for a screened potential is written as

$$T_{\mathrm{MC}}(\mathbf{k}',\mathbf{k};\varepsilon)\approx-2\pi g^+(Z^\infty,k',\varepsilon)g^+(Z^\infty,k,\varepsilon)\ f^C_{\mathbf{k}',\mathbf{k}}(\varepsilon) \quad (13)$$

where the scattering amplitude is

$$f^C_{\mathbf{k}',\mathbf{k}}(\varepsilon)\equiv\frac{2Z_s}{|\mathbf{k}'-\mathbf{k}|^2}\,e^{2i\sigma_0}\left[\frac{|\mathbf{k}'-\mathbf{k}|}{k'+k}\right]^{2i\nu_s} \quad (14)$$

and the off-shell factor is

$$g^\pm(Z^\infty,k,\kappa)=e^{\pi\nu^\infty/2}\Gamma(1\mp i\nu^\infty)\left[\frac{k-\kappa}{k+\kappa}\right]^{\mp i\nu^\infty}, \quad (15)$$

with $\nu_s=\mu Z_s/\kappa$, $\nu^\infty\equiv\mu Z^\infty/\kappa$, and $\kappa\equiv(2\mu\varepsilon+i\eta)^{1/2}$. The reduced mass is μ and $\Gamma(x)$ is the Gamma function. This simplification works for large impact energies and hard collisions (large momentum transfers).

Complete evaluation of the first Born amplitude in Eq. (4) gives [9]

$$A_{B1}=-4\pi^3(K^2+Z_P^2)[\tilde{\phi}_f(\mathbf{K})]^*\tilde{\phi}_i(-\mathbf{J}), \quad (16)$$

with $i=f=1s$. Applying the near-shell approximation to the electronic-nuclear transition matrices in $A_e^{(2)}$, neglecting the slowly varying $\mathbf{k}_i$ and $\mathbf{k}_f$ dependencies of the integrand, and introducing the $1s$ bound-state wave function in momentum space, $\tilde{\phi}_{1s}(\mathbf{k})=(2^3Z^5)^{1/2}/\pi(k^2+Z^2)^2$, the amplitude takes the form

$$A_e^2=2(2/\pi)^3Z_P(Z_TZ_P)^{5/2}e^{\pi\nu_P^\infty}\frac{\Gamma(1+i\nu_P^\infty)^2\Gamma(1-i\nu_P)}{\Gamma(1+i\nu_P)}(4v^2)^{i(2\nu_P^\infty-\nu_P)}K^{-2+2i\nu_P}e^{\pi\nu_T^\infty}|\Gamma(1+i\nu_T^\infty)|^2(4v^2)^{2i\nu_T^\infty}\left\{\frac{Z_s}{J^2}\left(\frac{J}{2v}\right)^{2i\nu_s}\right\} \times\int d\mathbf{k}_f d\mathbf{k}_i\ (k_i^2-2\varepsilon_i)^{-2-i\nu_P^\infty}\ (k_f^2-2\varepsilon_f)^{-2-i\nu_T^\infty}\ [\tilde{G}_Q^+(E_i)]^{1+i\nu_T^\infty+i\nu_P^\infty}. \quad (17)$$

The Sommerfeld parameters in this equation are defined as

$$\nu_P^\infty = Z_P^\infty/v, \quad \nu_P = Z_P/v, \quad \nu_T^\infty = Z_T^\infty/v, \quad \nu_T = Z_T/v. \tag{18}$$

A quadratic approximation

$$\tilde{G}_Q^+(E_i) \equiv [\tfrac{1}{2}(v^2 - K^2 + \varepsilon_i) - \mathbf{k}_f \cdot \mathbf{J} + \mathbf{k}_i \cdot \mathbf{K} - \tfrac{1}{2}(k_i^2 + k_f^2) + i\eta]^{-1} \tag{19}$$

to the free Green function $\tilde{G}_o^+(E_i)$ [Eq. (7)] has been introduced: $(\mathbf{k}_i - \mathbf{k}_f)^2 \approx k_i^2 + k_f^2$. That is, consistent with the spherical symmetry of the bound-state wave functions, a uniform averaging of all $\mathbf{k}_f$ directions relative to $\mathbf{k}_i$ is assumed. The inclusion of the quadratic term gives a significantly better representation of the free Green function [10]. The six-dimensional integral in Eq. (17) is evaluated as in previous work [1]. The calculated cross sections were checked to assure better than four-digit accuracy.

Introducing the near-shell approximation to the transition matrices in the first- and second-order internuclear partial amplitudes [Eqs. (8), (9), and (11)], performing the integrations after retaining the momentum dependences only in those terms in which the variation is rapid [which it is not in Eqs. (10) and (12)], and regrouping various factors, one obtains the expression

$$A_n = S_{PT} f_n^C(J) + S_{TP} f_n^C(K) \tag{20}$$

where the internuclear scattering amplitude is defined as

$$f_n^C(Q) = -\frac{2Z_P Z_T}{Q^2} \frac{\Gamma(1+i\nu_{PT})}{\Gamma(1-i\nu_{PT})} \left(\frac{Q}{2\mu_n v}\right)^{-2i\nu_{PT}}. \tag{21}$$

The constants S_{PT} and S_{TP} are independent of J and K. The former is

$$S_{PT} = 2^5 \pi Z_P (Z_P Z_T)^{3/2} e^{-\pi\nu_{PT}^\infty} \frac{\Gamma(1-i\nu_{PT}^\infty)\Gamma(\frac{1}{2}-i\nu_{PT}^\infty)}{(1-i\nu_{PT}^\infty)\sqrt{\pi}} (4\mu_n v^2)^{-2i\nu_{PT}^\infty}$$
$$\times \left[Z_T^{2i\nu_{PT}^\infty}(v^2+Z_P^2)^{-2+i\nu_{PT}^\infty} - \tfrac{1}{2} Z_P^{2i\nu_{PT}^\infty} \frac{\Gamma(\frac{1}{2}+i\nu_P^\infty)\Gamma(1+i\nu_P^\infty)\Gamma(1-i\nu_P)}{(1+i\nu_P^\infty)\sqrt{\pi}\,\Gamma(1+i\nu_P)} [\tfrac{1}{2}(v^2-Z_T^2)]^{-1+i\nu_{PT}^\infty} \left(\frac{Z_T}{2v}\right)^{-2i\nu_P^\infty} v^{-2+2i\nu_P} \right] \tag{22}$$

and the latter is obtained by the interchange $P \leftrightarrow T$ in S_{PT}. The Sommerfeld parameters ν_T^∞, ν_T, ν_P^∞, and ν_P are given by Eqs. (18) and $\nu_{PT}^\infty = Z_P^\infty Z_T^\infty/v$ and $\nu_{PT} = Z_P Z_T/v$. The integral in the intermediate version of Eq. (8) has been evaluated by treating the two dominant peaks in the integrand at $\mathbf{k}_i = \mathbf{0}$ and $\mathbf{k}_i = \mathbf{v}$ as independent with the slow $\mathbf{k}_i$ variation of the other factors about the peaks being neglected. This is justified if the two peaks are well separated in momentum space, as is true for $v \gg Z_P$ and $v \gg Z_T$.

Equation (20) is symmetric in the two sets of charges and the momentum transfers. The dependence on K^{-2} and J^{-2} reflects the nuclear Coulomb scattering. Noteworthy is the appearance of two terms of opposite sign in the large square brackets in Eq. (22). Ignoring the different multiplying factors and neglecting factors of order $(Z_P/v)^2$ and $(Z_T/v)^2$, a cancellation of contributions is expected in Eq. (20). It may be noted once again that the second Born approximation does not give an internuclear contribution at high velocities and forward angles ($S_{PT} \to 0$ and $S_{TP} \to 0$).

B. Eikonal transformation of the electronic amplitude

The eikonal treatment of the internuclear contribution to forward-angle capture transforms the transverse internuclear motion in the wave picture to a form dependent on a quantity analogous to the classical impact parameter [6]. Mathematically, it involves Bessel transforming the given electronic amplitude $A_e(K_\perp)$ [Eqs. (16) and (17)], as a function of transverse momentum transfer $K_\perp$, to impact parameter space b:

$$a_e(b) = \int_0^\infty dK_\perp K_\perp J_0(bK_\perp) A_e(K_\perp), \tag{23}$$

multiplying $a_e(b)$ by the eikonal phase factor $b^{2i\nu_{PT}}$, and then transforming the result back to momentum-transfer space

$$A_{e+n}(K_\perp) = \int_0^\infty db\, b^{1+2i\nu_{PT}} J_0(K_\perp b) a_e(b), \tag{24}$$

where ν_{PT} is the previously defined internuclear Sommerfeld parameter.

The notation A_{e+n} denotes that the electronic *and* internuclear contributions are intertwined in one amplitude. This manner of treatment of the internuclear contribution is apparently radically different from that given by the *sum* of amplitudes $A_e + A_n$ in the Faddeev treatment Eq. (1). In general, it appears that the two methods would not give similar amplitudes for *all* pertinent $K_\perp$ values, but only so when $A_n \gg A_e$. However, at sufficiently high velocities one notes that

$$b^{2i\nu_{PT}} \approx 1 + 2i\nu_{PT} \ln b + O((\nu_{PT})^2). \tag{25}$$

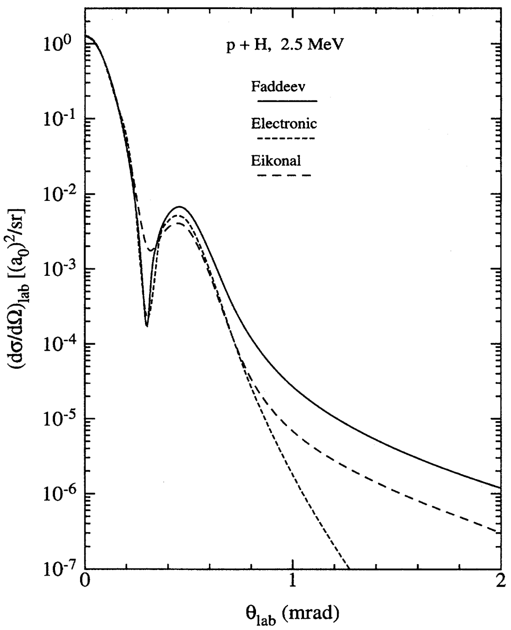

FIG. 1. Comparison of cross sections for charge transfer in 2.5-MeV proton-hydrogen collisions calculated using the full Faddeev amplitude, an eikonally transformed electronic Faddeev amplitude, and the electronic Faddeev amplitude. The impact velocity is ten times the characteristic velocity of the target electron.

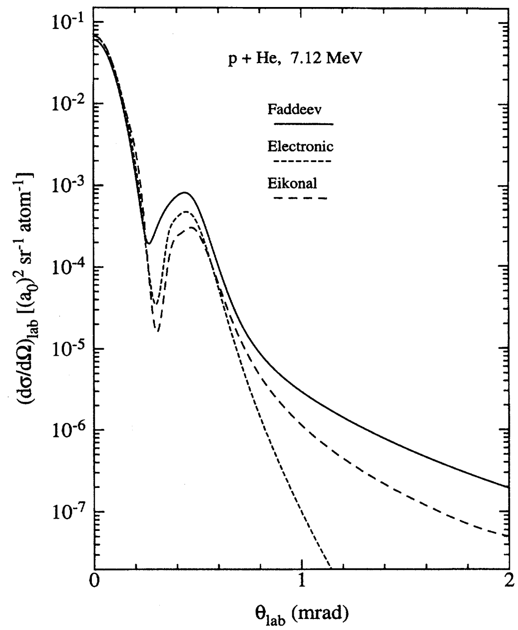

FIG. 2. Comparison of cross sections for charge transfer in 7.12-MeV proton-helium collisions calculated using the full Faddeev amplitude, an eikonally transformed electronic Faddeev amplitude, and the electronic Faddeev amplitude. The impact velocity is ten times the characteristic velocity of the target electron.

Thus the eikonal treatment reduces to something akin to the separable Faddeev result, provided the relevant b values are not too small or large—a reasonable assumption for protons on hydrogen or helium. Also, the approximate form on the right hand side (neglecting second- and higher-order terms) produces a convergent result because the complete integrand is well behaved in both the small and large b limits.

Normalization of the double integration in Eqs. (23) and (24) must be consistent with the definition of the amplitude relative to its use in the differential cross section. This is easily checked by setting $\nu_{PT}=0$ and comparing the doubly transformed amplitude with the untransformed amplitude, a procedure which also provides a gauge of the accuracy of the numerical quadratures. A further check on the errors deriving from the imperfectly calculated amplitude, which is read in at a tabulated set of values, is accomplished by performing the double numerical quadrature with the analytic function $\{c+K_\perp^2\}^{-2}$ [11].

C. Leading-order expression for the internuclear amplitude

The asymptotic expression for the internuclear amplitude is obtained by expanding in the ratios of the nuclear charges (and their product) to the impact velocity. Noting that $\Gamma(\frac{1}{2}+i\nu)=\pi^{1/2}[\Gamma(1+2i\nu)/2^{2i\nu}\Gamma(1+i\nu)]$ and $\ln\Gamma(1+i\nu)=-i\gamma\nu+\sum_{n=1}^{\infty}(-i\nu)^n\zeta(n)/n$, one has $\Gamma(1+i\nu)\Gamma(\frac{1}{2}+i\nu)\approx\pi^{1/2}2^{-2i\nu}(1-2i\nu)$ [12]. Using $\arg\Gamma(1+i\nu)=-\gamma\nu+\sum_{n=0}^{\infty}\sum_{i=1}^{\infty}[(-1)^{i-1}/2i+1][\gamma/(n+1)]^{2i+1}$, one finds $\Gamma(1-i\nu)/\Gamma(1+i\nu)=e^{-2i\arg\Gamma(1+i\nu)}\approx 1+2i\gamma\nu$. The quantity $\gamma=0.577\,21$ is Euler's constant. Thus, expanding the factors multiplying the internuclear scattering amplitude to first order in ν_{PT}, ν_{PT}^{∞}, ν_T, ν_T^{∞}, ν_P, and ν_P^{∞}, one obtains from Eqs. (20), (22), and the corresponding one for S_{TP} the asymptotic expression

$$\begin{aligned} A_n\approx i\,\frac{2^4\pi(Z_PZ_T)^{5/2}}{v^4}\,f_n^C(Q)\Bigg\{&2\left(\frac{1}{Z_P}-\frac{1}{Z_T}\right)\ln\left(\frac{Z_P}{Z_T}\right)\nu_{PT}^{\infty}\\ &+\frac{\nu_P^{\infty}}{Z_T}\left[1+2\gamma\left(1-\frac{Z_P}{Z_P^{\infty}}\right)+2\ln\left(\frac{Z_T}{v}\right)\right]\\ &+\frac{\nu_T^{\infty}}{Z_P}\left[1+2\gamma\left(1-\frac{Z_T}{Z_T^{\infty}}\right)+2\ln\left(\frac{Z_P}{v}\right)\right]\Bigg\}, \end{aligned} \tag{26}$$

where

$$f_n^C(Q)\approx-\frac{2Z_PZ_T}{Q^2}\left(\frac{Q}{2\mu_n v}\right)^{2i\nu_{PT}}(1-2i\gamma\nu_{PT}). \tag{27}$$

Equation (26) is symmetric in the appearance of the nuclear and asymptotic charges, including the first term in braces since $-\ln(Z_P/Z_T)=\ln(Z_T/Z_P)$. It is noteworthy that the two terms in Eq. (26) which vanish when $Z_P^{\infty}=Z_P$ and $Z_T^{\infty}=Z_T$ derive from *Coulomb* off-shell scattering.

For a symmetric collision where $Z_P=Z_T\equiv Z$, Eq. (26) reduces to

$$A_n\approx i\,\frac{2^5\pi Z^5}{v^4}\,f_n^C(Q)\,\frac{\nu^{\infty}}{Z}\left[1+2\gamma\left(1-\frac{Z}{Z^{\infty}}\right)+2\ln\left(\frac{Z}{v}\right)\right]. \tag{28}$$

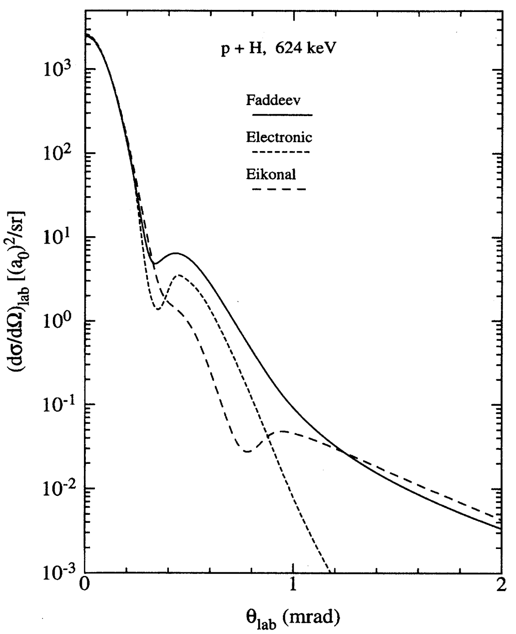

FIG. 3. Comparison of cross sections for charge transfer in 624-keV proton-hydrogen collisions calculated using the full Faddeev amplitude, an eikonally transformed electronic Faddeev amplitude, and the electronic Faddeev amplitude. The impact velocity is five times the characteristic velocity of the target electron.

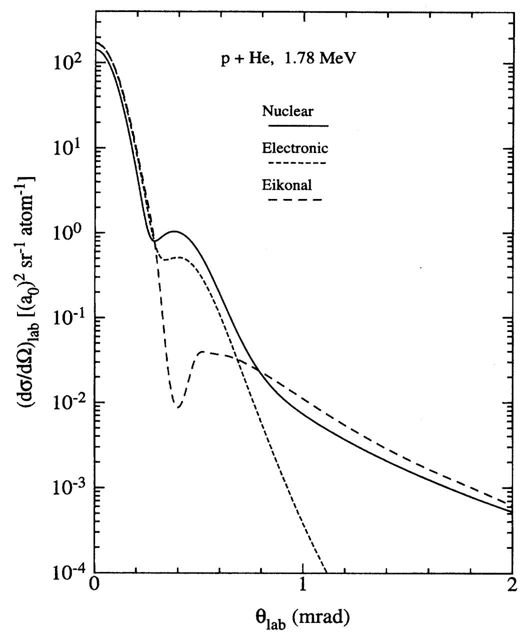

FIG. 4. Comparison of cross sections for charge transfer in 1.78-MeV proton-helium collisions calculated using the full Faddeev amplitude, an eikonally transformed electronic Faddeev amplitude, and the electronic Faddeev amplitude. The impact velocity is five times the characteristic velocity of the target electron.

If, further, the case of $Z^{\infty}=Z$ (e.g., protons on hydrogen) is considered, Eq. (26) becomes

$$A_n \approx i\,\frac{2^5 \pi Z^5}{v^5}\,f_n^C(Q)\left[1+2\ln\left(\frac{Z}{v}\right)\right]. \tag{29}$$

These limiting forms are reached, however, only very slowly as $v \rightarrow \infty$. In particular, Eq. (26) is not sufficiently accurate to be used at the energies employed in the present work.

IV. RESULTS AND DISCUSSION

Differential cross sections have been calculated using the second-order Faddeev approximation to the exact charge transfer amplitude [i.e., the sum of A_e in Eqs. (16) and (17) and A_n in Eq. (20)] and the eikonally transformed electronic amplitude [i.e., Eqs. (16) and (17) transformed according to Eqs. (23) and (24)]. Incident projectile velocities have been used which loosely represent the intermediate- and high-velocity regimes. Specifically, velocities of five and ten times the characteristic target orbital velocity are chosen. In the calculations, the values assumed for the charges in the Sommerfeld parameters are $Z_P= Z_P^{\infty}= Z_T= Z_T^{\infty}=1.0$ for protons on hydrogen and $Z_P= Z_P^{\infty}=1.0$, $Z_T=1.6875$, and $Z_T^{\infty}=1.0$ for protons on helium. The cross sections calculated using the Faddeev formalism exhibit a K^{-4} (or J^{-4}) momentum dependence in the region beyond 0.7 mrad, consistent with the Coulomb scattering of the projectile off the target nucleus and with Eq. (20).

The cross sections for $1s \rightarrow 1s$ charge transfer in proton-hydrogen collisions at 2.5 MeV and in proton-helium collisions at 7.12 MeV are presented in Figs. 1 and 2, respectively. These impact energies, which may be taken as representing the high-energy regime, correspond to velocities of ten times the characteristic target orbital velocities. The agreement between the Faddeev and eikonal cross sections is good up to 0.3 mrad. For the hydrogen case, the eikonal procedure washes out, substantially, the deep minimum in the electronic cross section whereas the Faddeev curve follows the electronic one; this behavior is reversed in the helium case. For both hydrogen and helium, the Faddeev result is somewhat larger in the Thomas peak region. The most surprising feature of Figs. 1 and 2 is that the Faddeev result is larger by a roughly constant amount. This aspect of the comparison is discussed below.

The cross sections for $1s \rightarrow 1s$ charge transfer in proton-hydrogen collisions at 0.624 MeV and in proton-helium collisions at 1.78 MeV are presented in Figs. 3 and 4, respectively. These intermediate impact energies correspond to velocities of five times the characteristic target orbital velocities. Considering the relatively lower velocity, the Faddeev and eikonal results agree rather well up to 0.3 mrad and beyond 1.0 mrad. From 0.3 to 1.0 mrad, however, the differences are quite large and are likely due to the interference between the first Born and second-order partial amplitudes. The origin of the localized dip in the eikonally transformed cross section, occurring at 0.75 mrad for protons on hydrogen and at 0.42 mrad for protons on helium, is unknown. A very similar dip occurs in results of the continuum distorted-wave theory (based on an entirely different theoretical framework) for protons on helium at 293 keV [13]. Such a dip

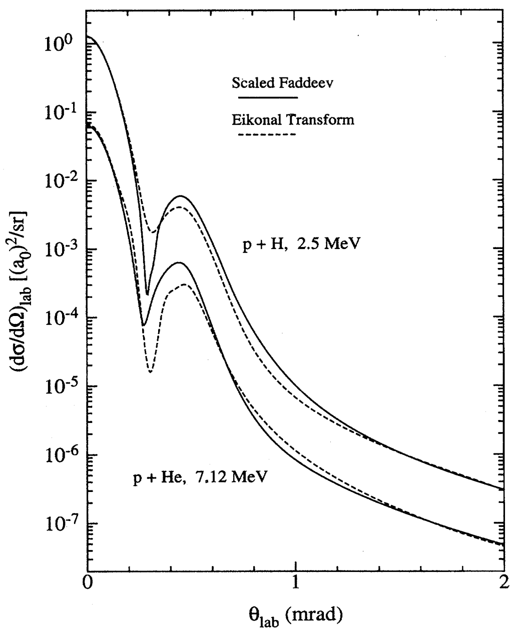

FIG. 5. Comparison of cross sections for charge transfer in 2.5-MeV proton-hydrogen and 7.12 MeV proton-helium collisions calculated using the full Faddeev amplitude scaled to the eikonally transformed electronic Faddeev amplitude at large angles, and the eikonally transformed amplitude.

seems to be a general feature of the eikonal procedure at intermediate velocities.

Though the differences at intermediate velocities are not unexpected, at higher velocities the differences at large angles seen in Figs. 1 and 2 are very puzzling. One would think that, of any angular and energy region, this is where agreement should occur. The differences can be clarified if the results are replotted with the Faddeev and eikonal results normalized to one another at large angles (say, 2.5 mrad). Figure 5 shows these results. This scaling affects only the nuclear part of the Faddeev amplitude as the electronic part is negligible there. The agreement of the scaled Faddeev and eikonal cross sections is then generally good. Certainly, the same total cross section would be obtained. The main remaining difference occurs where the electronic amplitude has the deep local minimum and the eikonal procedure fills this in. Also, there is still some difference in the Thomas peak region. Beyond 1.4 mrad, the two cross sections are identical in shape.

The ratio of the Faddeev results relative to the eikonal results for both hydrogen and helium, to good accuracy, is found to be 4. Thus a factor of 2 difference exists between the two amplitudes (actually, their moduli). Since the Faddeev theory contains *two* channels of internuclear scattering, represented by the two terms in Eq. (20), and the eikonal transformation builds on a single electronic amplitude, it appears that this difference in theories is the origin of the factor of 2 between the results at large angles.

In summary, it has been shown that the second-order Faddeev approximation to the transition operator for charge transfer at forward angles gives a differential cross section which varies considerably from the eikonally transformed one. Since A_e exhibits a K^{-6} dependence at the larger angles, so that its contribution can be neglected, it follows that the total cross section factors into the product of electronic and nuclear parts. The eikonal transformation of an electronic amplitude shows how the internuclear contribution can be represented though a multiplicative phase factor but at sufficiently high velocities a separation of the two can be effected as Eq. (25) shows. Finally, it has been shown that a multiple-scattering theory which includes two generalized Thomas mechanisms gives a factor of 4 increase (amplitude squared) in the internuclear contribution at large angles relative to the eikonal result.

ACKNOWLEDGMENTS

I thank J. H. Macek for discussion on the double contribution of the Faddeev amplitude and for his hospitality while on sabbatical at UT. This work is supported by the U.S. Department of Energy, Office of Energy Research, Office of Basic Energy Sciences, Division of Chemical Sciences. Calculations were performed on the Lawrence Livermore National Laboratory's Cray-2.

[1] S. Alston, Phys. Rev. A **42**, 331 (1990); K. Taulbjerg and J. S. Briggs, J. Phys. B **16**, 3811 (1983).

[2] E. Horsdal-Pedersen, C. L. Cocke, and M. Stockli, Phys. Rev. Lett. **50**, 1910 (1983); H. Vogt, R. Schuch, E. Justiniano, M. Schulz, and W. Schwab, *ibid.* **57**, 2256 (1986); T. R. Bratton, C. L. Cocke, and J. R. Macdonald, J. Phys. B **10**, L517 (1977).

[3] L. H. Thomas, Proc. R. Soc. London Ser. A **114**, 561 (1927); R. Shakeshaft and L. Spruch, Rev. Mod. Phys. **51**, 369 (1979); R. M. Drisko, Ph.D. thesis, Carnegie Institute of Technology, 1955; J. S. Briggs and K. Taulbjerg, J. Phys. B **12**, 2565 (1979).

[4] L. D. Faddeev, Zh. Eksp. Teor. Fiz. **39**, 1459 (1960) [Sov. Phys. JETP **12**, 1014 (1961)]; K. M. Watson, Phys. Rev. **88**, 1163 (1952); C. Lovelace, *ibid.* **135**, B1225 (1964).

[5] C. J. Joachain, *Quantum Collision Theory* (North-Holland, Amsterdam, 1975).

[6] R. McCarroll and A. Salin, J. Phys. B **1**, 163 (1968); J. S. Briggs, P. T. Greenland, and L. Kocbach, *ibid.* **15**, 3085 (1982).

[7] J. C. Y. Chen and A. C. Chen, Adv. At. Mol. Phys. **8**, 71 (1972); S. Alston, Phys. Rev. A **38**, 636 (1988); H. Marxer, S. Alston, and J. Briggs, Z. Phys. D **5**, 35 (1987), and references therein.

[8] S. Alston, Phys. Rev. A **38**, 3124 (1988).

[9] J. R. Oppenheimer, Phys. Rev. **31**, 349 (1928); H. C. Brinkman and H. A. Kramers, Proc. Acad. Sci. Amsterdam **33**, 973 (1930).

[10] S. Alston, Phys. Rev. A **38**, 6092 (1988).

[11] G. E. Forsythe, M. A. Malcolm, and C. B. Moler, *Computer Methods for Mathematical Computations* (Prentice-Hall, Englewood Cliffs, NJ, 1977), Chap. 5.
[12] *Handbook of Mathematical Functions*, Natl. Bur. Stand. (U.S.) Appl. Math. Ser. No. 55, edited by M. Abramowitz and I. A. Stegun (U.S. GPO, Washington, DC, 1964).
[13] R. D. Rivarola, R. D. Piacentini, A. Salin, and Dž. Belkić, J. Phys. B **13**, 2601 (1980).